ChemComm

Accepted Manuscript

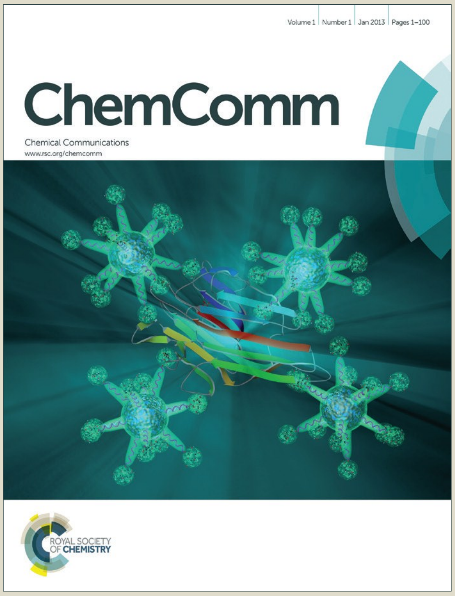

ROYAL SOCIETY OF CHEMISTRY

www.rsc.org/chemcomm

Journal Name

COMMUNICATION

Received 00th January 20xx,

Accepted 00th January 20xx

DOI: 10.1039/x0xx00000x

www.rsc.org/

Intramolecular electron transfer reactions in *meso*-(4-nitrophenyl)-substituted subporphyrins

Graeme Copley,[a] Juwon Oh,[b] Kota Yoshida,[a] Daiki Shimizu,[a] Dongho Kim[b,]* and Atsuhiro Osuka[a]

A_2B-type *meso*-(4-nitrophenyl)-substituted subporphyrins have been synthesized and shown to undergo very fast photoinduced intramolecular charge separation (CS) and charge recombination (CR) between the subporphyrin core and *meso*-4-nitrophenyl group in CH_2Cl_2 as probed by femtosecond time-resolved transient absorption spectroscopy. Red-shifted emissions were detected from charge-separated states as a rare case for porphyrinoids.

Since our initial report describing the synthesis of tribenzosubporphins in 2006,[1] much attention has been focused on the exploration of subporphyrins because of their attractive optical, electronic, and structural attributes.[2] A characteristic feature of subporphyrin that is not shared with its older cousin porphyrin is the facile rotation of *meso*-aryl substituents that allows them to exert large electronic influences on the subporphyrin core, drastically altering the properties of the subporphyrin.[3] Prime examples include *meso*-(4-aminophenyl)-substituted subporphyrins and *meso*-(4-oligo(phenylethynyl)-substituted subporphyrins, both of which exhibited perturbed optical and electrochemical properties.[4] Facile rotation of *meso*-aryl groups leads to twisted intramolecular charge transfer in subporphyrins bearing *meso*-arylamino groups.[5] Apart from these accounts, studies on electron transfer reactions of subporphyrins have been rather limited, while significant fluorescence quenching of subporphyrins has been observed in several cases.[6,7]

In this work, we have focused on a set of A_2B-type subporphyrins bearing *meso*-4-nitrophenyl groups (Fig. 1) paying particular attention to intramolecular electron transfer reactions. While *meso*-4-nitrophenyl-substituted subporphyrin was previously prepared and its significant fluorescence quenching in CH_2Cl_2 was noted,[7] the photo-excited-state dynamics were not examined in detail. In subporphyrins **1-3**, the 4-nitrophenyl groups are free to rotate at will, maximising their electronic influence on the subporphyrin core. However, the rotational freedom of the nitro groups in **2** and **3** is different, since the introduced methyl groups in **2** and **3** decrease the rotational freedom. In **4**, the 2-methyl group imposes a severe rotational barrier of the *meso*-aryl substituent, enforcing an orthogonal conformation.[8]

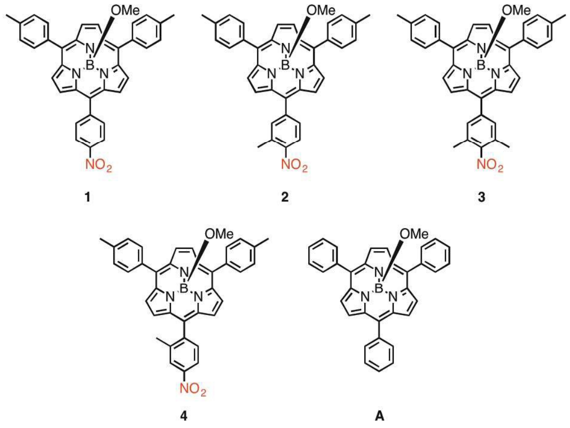

Fig. 1 The molecular structures of the subporphyrins described in this study.

Subporphyrins **1-4** were synthesized by following improved protocols for realizing A_2B type subporphyrins in 16, 8, 7, and 3% yields, respectively. The purity and authenticity of **1-4** have been unambiguously confirmed by ^{1}H, ^{11}B, ^{13}C NMR spectroscopy, and high-resolution atmospheric-pressure-chemical-ionization (HR-APCI-TOF) mass spectrometry (Figures S2 and S3 in ESI). The ^{1}H NMR spectrum of **4** displays signals corresponding to both *exo*- and *endo*-atropisomers in a 4:1 ratio in $CDCl_3$ at room temperature (Figure S2-10 in ESI). The ^{1}H NMR spectrum of compound **4** remained unchanged upon elevating to high temperatures, indicating a high rotational barrier of the 2-methyl-4-nitrophenyl substituent. Single crystals of **1** suitable for X-Ray diffraction analysis were

---

[a] *Department of Chemistry, Graduate School of Science, Kyoto University, Kyoto 606-8502, Japan.*
[b] *Department of Chemistry, Yonsei University, Seoul 120-749, Korea.*

Electronic Supplementary Information (ESI) available: [details of any supplementary information available should be included here]. See DOI: 10.1039/x0xx00000x obtained by slow diffusion of pentane in to a solution of **1** in benzene (Figure 2). The average bowl depth was calculated to be 1.34 Å[9], whilst the dihedral angle of the 4-nitrophenyl group was determined to be 41.97°. These values are consistent with the ground state optimized geometry (see below).

Using the crystal structure of **1** as a starting point, optimised ground state structures of **1**-**4** have been calculated using the *Gaussian 09* program package (Figure S8-1 in ESI). The dihedral angles of the *meso*-4-nitrophenyl groups in **1**-**3** were calculated to be 44.6°, 44.3°, and 45.2°, respectively, suggesting that the *meso*-4-nitrophenyl groups in **1**-**3** possess very similar rotational freedom.

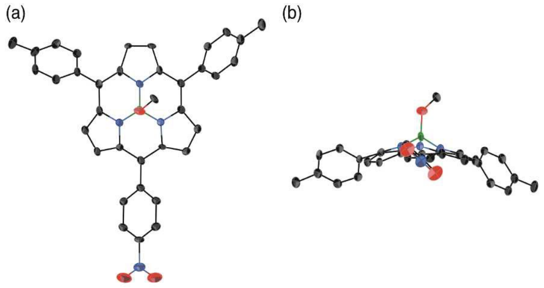

Fig. 2 X-Ray crystal structure of **1** (a: top view, b: side view). The molecular structure shown is one of two independent molecules in the unit cell. Thermal ellipsoids are set at 50% probability level. Hydrogen atoms and solvent molecules are omitted for clarity.

The dihedral angles between the nitro group and its respective aryl group in **1**-**3** were calculated to be 0.5°, 12.3°, and 42.9°, respectively. This ascending trend is in line with the systematic introduction of methyl groups adjacent to the nitro group, gradually increasing steric hindrance. As anticipated, the dihedral angle between the 2-methyl-4-nitrophenyl group and subporphyrin core was calculated to be 58.2°, much larger than the dihedral angles observed for **1**-**3** (44.6°, 44.2°, and 45.2°). This can be ascribed to the steric clash between the 2-methyl group and the subporphyrin periphery. The dihedral angle of the nitro group and its respective aryl group in **4** was calculated to be just 0.7°, indicating that a coplanar relationship is favoured as in the case of **1**. Despite their individual structural features, the molecular orbital diagrams calculated for **1**-**4** suggest that all of the compounds share a similar intramolecular charge transfer character (Figure S8-2 in ESI). In the HOMO plots for **1**-**4**, electron density is distributed over the entirety of the molecular framework. In the LUMO plots for **1**-**4**, electron density appears to be pulled on to the electron withdrawing *meso*-4-nitrophenyl substituents and away from the subporphyrin cores.

Fig. 3 shows the absorption and emission spectra of **1**-**4** along with reference compound triphenylsubporphyrin **A** in CH_2Cl_2 (an important observation to note is that the absorption spectra of **1**-**4** recorded in CH_2Cl_2 were practically the same as those recorded in toluene (Figure S7-1 in ESI)). The Soret-like band of **1** is the broadest in the set, indicating the largest electronic interaction between the 4-nitrophenyl group and subporphyrin core. There is a visible sharpening of the Soret-like band and overall absorption spectra moving through **1**-**3**, and a slight broadening again for **4**. The full width at half maximum (FWHM) values for **1, 2**, **3** and **4** are 2870, 2309, 1785, and 1993 cm^{-1}, respectively. This sharpening trend in **1**-**3** can be ascribed to the dwindling electronic influence of nitro group on the subporphyrin core due to increasing steric constraint. The λ_{max} value of 372 nm and molar extinction coefficient value of 1.50×10^5 M^{-1} cm^{-1} for **4** highlights the decoupled nature of the *meso*-2-methyl-4-nitrophenyl group and the subporphyrin core. In comparison to **3**, a slight broadening of the absorption profile for **4** is most likely due to the presence of its atropisomers.

Table 1 Photophysical parameters of compounds **1**-**4**. Values were recorded in CH_2Cl_2 unless stated.

comp.	λ_{max} / nm	FWHM / cm^{-1}	ε / M^{-1}cm^{-1}	Φ_F in CH_2Cl_2	Φ_F in toluene
1	378, 464, 493	2870	8.20×10^4	0.022	0.28
2	379, 464, 493	2309	1.22×10^5	0.040	0.26
3	375, 463, 489	1785	1.55×10^5	0.013	0.22
4	372, 460, 485	1993	1.50×10^5	<0.001	0.23
A	373, 461, 484	1527	1.66×10^5	0.14	0.16

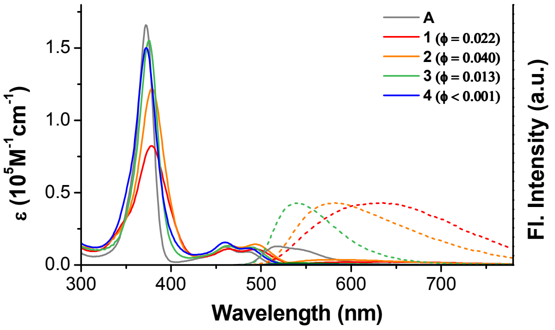

Fig. 3 Absorption (solid) and emission (dashed) spectra for compounds **1**-**4**, along with control compound **A**, recorded in CH_2Cl_2.

In non-polar toluene, the emission maxima for **1**-**4** were observed at 542, 546, 533, and 533 nm with the fluorescence quantum yields recorded as 0.28, 0.26, 0.22, and 0.23, respectively. Compared to **A**, increased fluorescence quantum yields of **1**-**4** suggests that a perturbation effect is introduced by the presence of the 4-nitrophenyl groups, where the higher quantum yields of **1** and **2** in comparison to **3** and **4** can be ascribed to the restricted influence of the nitro groups on the subporphyrin core in **3** and **4**. In contrast, the fluorescence emissions of **1**-**4** are all significantly quenched in moderately polar CH_2Cl_2 (0.022, 0.040, 0.013, and < 0.001 for **1**-**4**, respectively) with their fluorescence emission spectra becoming significantly broadened and red-shifted. Such spectral features suggest the occurrence of efficient intramolecular charge transfer processes in **1**-**4**. Again, a nice trend can be observed for the broadening and red-shifting of the emission profiles with respect to **1**-**3**, with **1** exhibiting the most broadened and most red-shifted emission profile.

Table 2 Redox potentials of **1**-**4** in CH_2Cl_2 measured by Cyclic Voltammetry[a] and estimated energy levels of CSS and $-\Delta G°$ for charge separation.

compound	$E^{1/2}_{OX1}$ / V	$E^{1/2}_{RED1}$ / V	$E^{1/2}_{RED2}$ / V	CSS / eV	$-\Delta G°$ (eV)
1	0.78	−1.36[b]	−1.56[b]	1.86	−0.49
2	0.72	−1.74		2.18	−0.19
3	0.70	−1.79		2.21	−0.21
4	0.71	−1.69	−1.96	2.12	−0.25
A	0.71	−1.97			

[a] Conditions: scan rate: 0.05 V/s, supporting electrolyte: 0.1 M $n\mathrm{Bu_4NPF_6}$, working/counter electrodes: Pt/Pt wire, reference electrode: Ag/0.01 M $AgClO_4$ in MeCN. [b] Determined by differential pulse voltammetry.

The electrochemical properties of **1**-**4** along with reference subporphyrin **A** were investigated by cyclic voltammetry (CV) measurements in CH_2Cl_2 and the results are listed in Table 2. The first oxidation waves of **1**, **2**, and **3** were observed at 0.78, 0.72, and 0.70 V, respectively, reflecting the decreasing influence of the nitro group due to the installed methyl groups, in this order. In the reduction part, **1** showed two reversible reduction waves at –1.36 V and –1.56 V. By searching the existing literature, these two reduction waves have been assigned to the reduction of the freely rotating 4-nitrophenyl group and of the electron deficient subporphyrin core, respectively.[10] In **2**, the installed methyl group mitigates communication between the nitro group and aryl group. Judging from the first oxidation and reduction potentials of 0.72 and –1.74 V, the nitro group in **2** is exerting a modest influence on the subporphyrin core. The influence of the nitro group in **3** is even less due to the two methyl groups flanking the nitro group. Finally, the oxidation potential of **4** was observed at 0.71 V, whilst the reduction potentials were observed at –1.69 and –1.96 V. These values confirm that the 2-methyl-4-nitrophenyl group in **4** is electronically decoupled from the subporphyrin core, although the nitro group can still influence its respective aryl group due to the absence of methyl groups at the 3 and 5 positions. On the basis of the above electrochemical data, the energy levels of the charge separated states (CSS), consisting of a subporphyrin cation radical and a nitrobenzene anion radical, have been estimated to be 1.86, 2.18, 2.21, and 2.12 eV for **1**-**4**, respectively (Coulombic correction term was taken into account when calculating these values (Table 2)). These considerations made it possible to estimate the driving force for CS to be –0.49, –0.19, –0.21, and –0.25 eV for **1**-**4**, respectively.

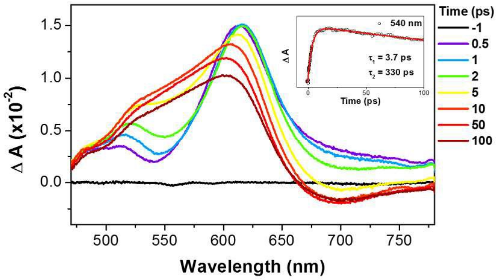

Fig. 4 TA spectra and decay profile (inset) of **1** in CH_2Cl_2 (excitation at 490 nm).

To reveal the CS and CR events in **1**-**4**, femtosecond transient absorption (TA) spectra were recorded in CH_2Cl_2 (Figures 4 and S7-2 in ESI). As a control experiment, a subporphyrin cation radical generated by chemical oxidation of **A** with $NOSbF_6$ displayed absorption bands at 388 and 502 nm (Figure S6-1 in ESI). After searching the literature, the electrochemically generated radical anion of nitrobenzene showed absorption bands at 435 and 465 nm with a tail reaching out to 600 nm.[11] The TA spectra of **1** displayed a very rapid formation and decay of the CS state showing broad absorbance in the range of 500–630 nm consisting of contributions from subporphyrin cation radical and nitrobenzene anion radical with a CS rate of $(3.7\ \mathrm{ps})^{-1}$ and a CR rate of $330\ \mathrm{ps}^{-1}$. The TA spectra of **2** and **3** also revealed quantitative CS and CR with $k_{CS} = (3.0\ \mathrm{ps})^{-1}$ and $k_{CR} = (530\ \mathrm{ps})^{-1}$ for **2**, and $k_{CS} = (2\ \mathrm{ps})^{-1}$ and $k_{CR} = (210\ \mathrm{ps})^{-1}$ for **3**, respectively. The fluorescence lifetimes of **1**-**3** (340, 510, and 200 ps, respectively) were all well matched with the lifetimes for CR processes, indicating that their red-shifted fluorescence in CH_2Cl_2 is originating from the CS state (Figure S7-3 in ESI). It is worthy to note that such CR-associated emissions[12] have been very rare for porphyrins. The TA spectra of **4**, which is held in an orthogonal conformation, also indicated rise and decay of broad absorbance in the range of 480 nm and 660 nm due to the CS state with $k_{CS} = (5.0\ \mathrm{ps})^{-1}$ and $k_{CR} = (40\ \mathrm{ps})^{-1}$. Very fast CR in **4** may explain its non-fluorescent nature in the red-shifted region due to its short lived CS state. Therefore, it may be inferred that weak CR-associated emission is only allowed for subporphyrins bearing freely rotating *meso*-aryl groups.

In summary, A_2B-type *meso*-(4-nitrophenyl)-substituted subporphyrins **1**-**4** have been synthesized and have been shown to undergo very fast photoinduced intramolecular CS and CR reactions between the subporphyrin core and *meso*-4-nitrophenyl group in CH_2Cl_2. Characteristically, broad and red-shifted emissions were detected from the CS states of **1**-**3** as a rare case for porphyrinoids.

The work at Kyoto was supported by JSPS KAKENHI Grant Numbers (25220802 and 25620031). The work at Yonsei was supported by Global Research Laboratory (GRL) Program (2013K1A1A2A02050183) through the National Research Foundation of Korea (NRF) funded by the Ministry of Science, ICT (Information and Communication Technologies) and Future Planning. GC thanks JSPS for a Postdoctoral Fellowship.

Notes and references

1 Y. Inokuma, J. H. Kwon, T. K. Ahn, M.-C. Yoo, D. Kim and A. Osuka, *Angew. Chem. Int. Ed.* 2006, **45**, 961.

2 a) T. Torres, *Angew. Chem. Int. Ed*. 2006, **45**, 2834; b) Y. Inokuma and A. Osuka, *Dalton Trans*. 2008, 2517; c) A. Osuka, E. Tsurumaki and T. Tanaka, *Bull. Chem. Soc. Jpn.* 2011, **84**, 679; d) C. G. Claessens, D. González-Rodríguez, M. S. Rodríguez-Morgade, A. Medina and T. Torres, *Chem. Rev.* 2014, **114**, 2192; N. Kobayashi, Y. Takeuchi, A. Matsuda, *Angew. Chem. Int. Ed.* 2007, **46**, 758.

3 Y. Inokuma, Z. S. Yoon, D. Kim and A. Osuka, *J. Am. Chem. Soc.* 2007, **129**, 4747.

4 a) Y. Inokuma, S. Easwaramoorthi, S. Y. Jang, K. S. Kim, D. Kim and A. Osuka, *Angew. Chem. Int. Ed.* 2008, **47,** 4840; b) Y.

Inokuma, S. Easwaramoorthi, Z. S. Yoon, D. Kim and A. Osuka, *J. Am. Chem. Soc.* 2008, **130**, 12234.

5 M. Kitano, S. Hayashi, T. Tanaka, N. Aratani and A. Osuka, *Chem. Eur. J.* 2012, **18**, 8929; b) W.-Y. Cha, J. M. Lim, K. H. Park, M. Kitano, A. Osuka and D. Kim, *Chem. Commun.* 2014, **50**, 8491.

6 a) H. Sugimoto, T. Tanaka and A. Osuka, *Chem. Lett.* 2011, **40**, 629: b) S. Saga, S. Hayashi, K. Yoshida, E. Tsurumaki, P. Kim, Y. M. Sung, J. Sung, T. Tanaka, D. Kim and A. Osuka, *Chem. Eur. J.* 2013, **19**, 11158; c) D. Shimizu, H. Mori, M. Kitano, W.-Y. Cha, J. Oh, T. Tanaka, D. Kim and A. Osuka, *Chem. Eur. J.* 2014, **20**, 16194.

7 T. Tanaka, M. Kitano, S. Hayashi, N. Aratani and A. Osuka, *Org. Lett.* 2012, **14**, 2694.

8 K. Yoshida, G. Copley, H. Mori and A. Osuka, *Chem. Eur. J.* 2014, **20**, 10065.

9 The bowl depth of subporphyrin is defined as the vertical distance between the mean plane of the six β carbon atoms and the central boron atom.

10 A. Kuhn, K. G. von Eschwege and J. Conradie, *J. Phys. Org. Chem.* 2012, **25**, 58.

11 W. Kemula and R. Sioda, *Nature* 1963, **197**, 588.

12 a) P. Pasman and J. W. Verhoeven, *J. Am. Chem. Soc.* 1982, **104**, 5127; b) P. Pasman, G. F. Mes, N. W. Koper and J. W. Verhoeven, *J. Am. Chem. Soc.* 1985, **107**, 5839.